Trop J Nat Prod Res, March 2023; 7(3):2586-2595 ISSN 2616-0684 (Print)
ISSN 2616-0692 (Electronic)

Tropical Journal of Natural Product Research

Available online at https://www.tjnpr.org

Original Research Article

Screening Indonesian Pine (*Pinus merkusii* Jungh at de Vriese) Compound as an Antibacterial Agent: *In Vitro* and *In Silico* Study

Yuka Fadana[1], Ichda A. Dinana[2], Arie Srihardyastutie[1], Rollando Rollando[3], Masruri Masruri[1,*]

[1]*Chemistry Department, Faculty of Mathematics and Natural Sciences, Brawijaya University, Malang 65145, Indonesia,*
[2]*Biology Department, Faculty of Mathematics and Natural Sciences, Brawijaya University, Malang 65145, Indonesia,*
[3]*Pharmacy Department, Faculty of Science and Technology, Ma Chung University, Malang 65151, Indonesia*

ARTICLE INFO

Article history:
Received 11 February 2023
Revised 23 March 2023
Accepted 24 March 2023
Published online 01 April 2023

ABSTRACT

Pinus merkusii is empirically used as an antibacterial agent and has been found to have secondary metabolites such as alkaloids, terpenoids, and flavonoids. This study aims to investigate the antibacterial effects of pine flower extract on gram-positive and gram-negative bacteria. In addition, molecular docking and molecular dynamics simulations were used to understand the underlying mechanism of its antibacterial activity. The antibacterial screening was performed using the disc diffusion method, compound analysis in the extract was carried out using Liquid Chromatography-Tandem Mass Spectrometry (LC-MS/MS), molecular docking was performed using Autodock Vina integrated into PyRx, and molecular dynamics simulation was run using YASARA Dynamics. The antibacterial test results showed that the pine flower extract had the highest inhibitory effect on *Escherichia coli* (1.038 ± 0.169 mm) and *Staphylococcus aureus* (7.154 ± 0.381 mm). Compound analysis of the pine flower extract showed the presence of Myricetin, Epicatechin, Nepetin, Hispidulin, Kaempferol, Luteolin-7-*O*-rutinoside, and Hesperidin. The molecular docking and molecular dynamics simulation results showed that Epicatechin, Nepetin, and Luteolin-7-*O*-rutinoside compounds could inhibit bacterial cell wall formation proteins.

Keywords: antibacterial; pine, *Staphylococcus aureus*, *Escherichia coli*, *in-silico*

Introduction

Serious diseases due to bacterial infection are still one of the world's biggest concerns.[1] In many cases, antibacterial drugs can have various side effects and may be hard to find in some remote areas.[2] A quick and effective solution such as research on new drug compounds is urgently needed to support drug needs. Apart from the synthesis in the laboratory, medicinal compounds can also be obtained from the isolation of secondary metabolites from plants.[3] Several developed nations employ secondary plant metabolites for their anti-inflammatory, antibiotic, antifungal, anticancer, and antibacterial properties.[4] Pine (*Pinus merkusii* Jungh et de Vriese) is a plant that produces secondary metabolites.[5] Several studies related to pine mentioned some common content in this plant including alkaloids, phenolic compounds, flavonoids, tannins, terpenes, saponins, and many more.[6] Pine is often used as a traditional medicine in several countries as a medicine for pain, inflammation, digestive disorders, and even wound healing. Some of the diseases above are diseases caused by microbes.[7]

Each of these bacteria has a protein associated with their body's metabolism. Antibacterial agents are targeted as chemical interventions or mimic anti-bacterial resistance mechanisms.[8] Some targets of antibacterial drugs are affecting the biosynthesis of bacterial cell walls, biosynthesis of bacterial proteins, destroying bacterial cells, and replicating bacterial DNA.[9]

*Corresponding author. E mail: masruri@ub.ac.id
Tel: +62 82142017342

Citation: Fadana Y, Dinana IA, Srihardyastutie A, Rollando R, Masruri M. Screening Indonesian Pine (*Pinus merkusii* Jungh at de Vriese) Compound as an Antibacterial Agent: In Vitro and In Silico Study. Trop J Nat Prod Res. 2023; 7(3):2586-2595 http://www.doi.org/10.26538/tjnpr/v7i3.19

Official Journal of Natural Product Research Group, Faculty of Pharmacy, University of Benin, Benin City, Nigeria

The test bacteria that represent the conditions of ownership of gram-positive and negative are *Staphylococcus aureus* and *Escherichia coli,* respectively.[10] In bacteria *S. aureus* has TyrRS protein which is used in catalyzing tyrosine in ATP formation and C30 protein which produces aureus pigment in reducing survival under oxidative stress conditions.[12,13] Additionally, D-alanyl-D-alanine ligase, which regulates autolysin activity to maintain cation homeostasis, and protein gyrase-B, a bacterial enzyme that catalyzes the ATP-dependent negative supercoiling of double-stranded closed-circular DNA, are present in *E. coli*.[13,14] The aforementioned proteins are the main focus of antibacterial agents in interfering with the nucleic acid structure of bacteria.[15]

This research focuses on studying the compound components in pine and its antibacterial activity by inhibiting nucleic acid proteins from bacteria. Instruments validated the determination of the compounds contained in pine and the antibacterial properties of the metabolite compounds were validated by positive control of amoxicillin through in vitro and in silico mechanisms.

Material and Methods

Sample preparation and extraction

The study utilized various parts of the pine tree, including leaves, bark, twigs, and flowers, gathered from sector 9 of the UB forest in the Karangploso District of Malang Regency. The samples were collected in January 2022 and were assigned a voucher number, UB19233. A

powdered sample was prepared by grinding the samples for later extraction using maceration techniques. Powdered samples were weighed in a 1:4 (w/v) ratio and soaked for 3x24 hours using ethanol.[16] The sample was separated from the liquid extract using a funnel. The liquid extract was later condensed using a rotary evaporator.

In vitro Antibacterial assay

The disc diffusion method was used to conduct an antibacterial activity assay. Condensed pine extract (ethanol) diffused using 100% dimethyl sulfoxide (DMSO) into 200 mg/mL concentrations with 8 repetitions.[17] The negative control was DMSO, and the positive control was amoxicillin. *Staphylococcus aureus* and *Escherichia coli* bacterial cultures were diffused on Natrium Broth (NB) media with a total cell density of 10^6 cells/mL.[18] Diffused bacterial cultures were then aseptically spread with a cotton swab on a Natrium Agar (NA) medium prepared in a labeled petri dish. The blank disk was then soaked in different pine extract concentrations (1000; 500; 250; 125; 62,5 µg/mL) and placed in each labeled area. The dish was incubated for 24 hours at 37°C. The clear area around the disk was measured using a digital micrometer for antibacterial activity.[10]

Compound component assay

The concentrated extract was vortexed for 1 minute, filtered with a millipore, and injected into an autosampler. Analysis using LC-MS/MS was carried out to determine the molecular weight and name of the compound extracted from the pine plant using ethanol as a solvent. The dominant compound with the most significant area was taken from the generated data. Molecular structure analysis was carried out by predicting the similarity of the mass spectra of the compound with the mass spectra of the library compound. Compounds with a similarity value (Best similar match) are taken above 90.[19]

In-silico Antibacterial assay

Prediction of drug-likeness was performed using SwissADME to predict the suitability of the compound as a drug candidate, while potential biological activities were examined using PASS-online,[20] the quality of the compound was indicated by Pa value, higher Pa value implies higher bioactivity resemblance to known drugs in the PASS training set.[21]

The compounds identified by the LCMS/MS were subsequently downloaded from PubChem. Minimized the energy of all retrieved 3D structures using PyRx open babel tool.[22] The bacterial proteins used were tyrosyl-tRNA synthetase (TyRS) (PDB ID 1JIL) and C30 carotenoid dehydrosqualene synthase (PDB ID 3NPR) from Staphylococcus aureus, gyrase-B (PDB ID 6YD9) and D-alanyl-D-alanine ligase (DDl) (PDB ID 4C5A) from *Escherichia coli*. Protein 3D structures collected from RCSB PDB were prepared using Biovia Discovery Studio by removing the native ligand and water molecules.[23] The positive control used was Amoxicillin.[24]

Molecular docking analysis was performed using Autodock Vina integrated into PyRx. Amoxicillin as the positive control was blindly docked first to find the binding area, while the selected compound was docked specifically following the grid areas listed in Table 1.[25]

Molecular Dynamic Simulation run under Microsoft Windows 10 operating system, Molecular Dynamics (MD) simulation was performed using YASARA Structure version 14.12.2.[26] The YAMBER Force field was utilized in this simulation. The Ewald particle algorithm is used to determine the Coulomb distance interaction, while the Van der Waals force is constrained to 8. At a distance of 5 nm, a cube-shaped simulation box is positioned around the simulated molecules.[27] The simulated box has dimensions of 50x50x50 Å and a n value of 6. The boundary of the virtual box is subject to periodic conditions. At 298 K, the water's density was set to 1 g/cc.[28] Photos were shot every 100 ps7 while simulations were running for 20 ns.[25]

Table 1: Specific Search Area Used for Docking

No	Bacteria	Protein	Center			Dimension		
			X	Y	Z	X	Y	Z
1	*S. aureus*	TyRS	34.17	13.20	82.68	14.69	11.21	17.76
		C30	25.13	-13.85	7.48	15.33	19.21	9.37
2	*E. coli*	GyrB	9.27	-2.23	12.48	11.56	7.88	16.78
		DD1	16.25	21.13	60.92	12.22	12.36	15.66

Result and Discussion

The compounds (Table 2) isolated with 96% ethanol from the bark were 35.7 grams, twigs 29.2 grams, flowers 42.1 grams, and leaves 31.8 grams. It can be shown that the highest yield was in pine flowers. In general, plants produce secondary metabolites in vital parts aimed at protecting them from the environment, one of which is in the flower part, namely as part of the fertilization of a plant.[29]

In vitro Antibacterial assay

Bacterial culture inhibition from the disc diffusion method was analyzed by measuring the clear area around the disc that was previously soaked to the tested extract. From all tested parts, the pine flower showed the best antibacterial effect indicated by a large inhibition area (Table 3). All the tested extracts showed significant inhibition of *S. aureus* bacterial culture, as demonstrated by a large inhibition area. On the other hand, only the bark and flower extracts showed inhibition of the *E. coli* culture, with a small to no inhibition zone recorded. The diameter of the growth inhibition zone for *S. aureus* ranged from 5.1mm to 7.1mm, which was significantly larger than the inhibition zone recorded for *E. coli*, which measured only 1mm or less. These results signify that *S. aureus* is susceptible to pine extract as an expected antibacterial agent candidate. *S. aureus* are gram-positive bacteria, though having thick peptidoglycan layer, it has no supporting outer layer consisting of lipopolysaccharide (LPS) unlike its gram-negative relatives.[30] Hydrophobic drug can penetrate easily through diffusion pathway, while the hydrophilic drug that pass through porins and vancomycin will find it hard to penetrate gram-negative bacteria outer membrane due to its complex structure, thus gram-negative bacteria tend to be more resistant to several antibiotics than gram-positive.[31]

Table 2: Pine Extract Ethanol Solvent Yield

No.	Sample	Initial mass (g)	Extraction mass (g)	% Yield
1	Bark	300	35.7	11.90
2	Twig	300	29.2	9.70
3	Flower	300	42.1	14.03
4	Leaf	300	31.8	10.60

Table 3: Inhibition Zone from Disc Diffusion Test Formed by Pine Extract Treatment

No.	Sample	Growth inhibition (mm)	
		Escherichia coli	*Staphylococcus aureus*
1	Bark	1.071 ± 0.181	5.743 ± 0.518
2	Twig	0	5.145 ± 0.376
3	Flower	1.038 ± 0.169	7.154 ± 0.381
4	Leaf	0	7.150 ± 0.129

Compound analysis

Separation and identification using LC-MS/MS instrumentation showed several compounds identified from the chromatogram (Figure 1) of pine flower parts including Myricetin, Epicatechin, Nepetin, Hispidulin, Kaempferol, Luteolin-7-O-rutinoside, and Hesperidin (Table 4). All extracted compounds were classified as flavonoids, known for their activity as antibacterial agents against various pathogenic microorganisms.[32] Flavonoids as a plant-derived natural compound offer new possibilities as a substitute for antibiotics for their high availability, low toxicity, and effectiveness against antibiotic-resistant bacteria.[33]

In silico Antibacterial assay

Druglikeness prediction

The drug-likeness assay was conducted to determine whether the compound extracted from pine components possesses drug-like properties according to the Lipinsky Rule of 5 (LRO5) parameters. The LRO5 parameters include molecular weight less than 500 Da, hydrogen bond donors ≤ 5, hydrogen bond acceptors ≤ 10, and log P ≤ 5, and compounds adhering to these parameters are more likely to be absorbed by the body and less likely to cause harmful side effects. Compounds that violate more than one LRO5 parameter were excluded from further analysis for drug development, as Lipinsky suggested that an orally active drug should have fewer than two violations. Myricetin, which only violates one parameter (6 H-bond donors), is still considered a valid drug candidate. The drug-likeness prediction results indicated that all compounds, except for Hispidulin and Luteolin-7-O-rutinoside, have fewer or no LRO5 violations and are thus suitable candidates for drug development (Table 5).

Bioactivity prediction was carried out to predict the possible biological activity(s) of *P. merkusii* compounds. The selected activity presented in Figure 2 was narrowed down from several activities predicted regarding the ability of the compound to suppress or cease bacterial growth. The probable activities were ranked based on the probability of activity (Pa) value. The compounds were expected to show a specific activity when the Pa value is >0.71. Pass Online Pa Value was defined based on the molecular structure similarity of a typical active sub-set between the tested compound and the PASS training set compound.[21] The Pa value of a compound is indicated by the color, the darker the color, the higher the Pa Value (Figure 2). Myricetin presented the highest Pa value compared to other tested compounds as a peroxidase inhibitor and antimutagenic with Pa Value 0.966 and 0.963 respectively. Interestingly, although the Pa value for direct antibacterial activity is considerably low, the indirect activity that interferes with bacterial growth is noticeably high. A bioactivity prediction for flavonoids extracted from *P. merkusii* (Figure 2) showed that they are likely to possess antimutagenic properties, thus preventing bacterial resistance.

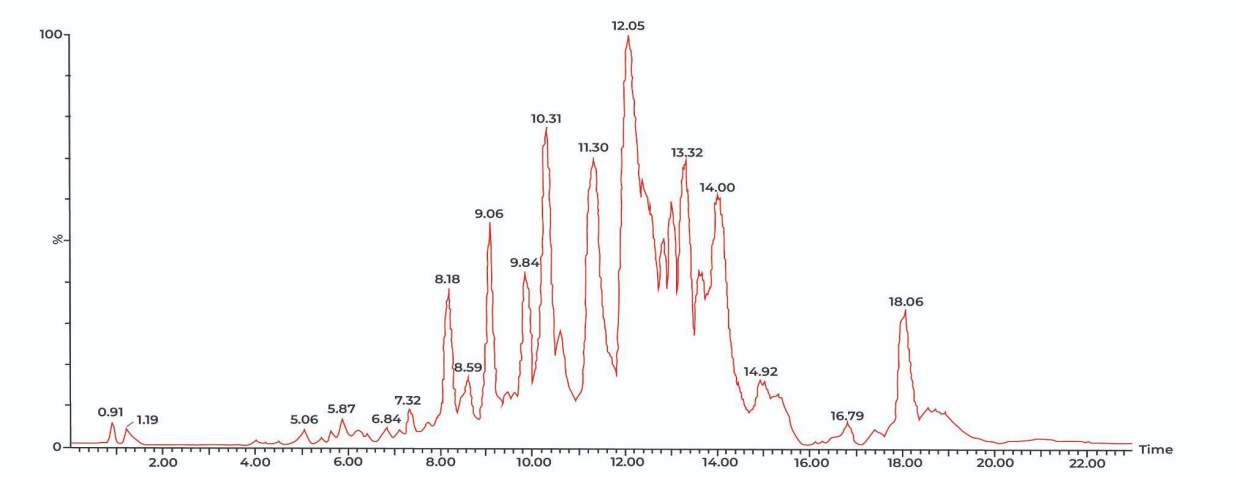

Figure 1: Liquid Chromatography Spectra Pine Flower Extract

Molecular docking analysis

Molecular docking was performed to analyze the activity of the potential compound extracted from *P. merkusii* as an antibacterial agent for both *Staphylococcus aureus* and *Escherichia coli*. The docking result against the key bacterial protein visualizes the same interacting pattern of all tested compounds compared to amoxicillin as the most commonly used antibiotic in primary health care (Figure 3), most of them possess higher binding affinity (Table 6). Various interactions were observed between the seven extracted compounds and the target proteins with no single compound dominating the docking results. Same interacting amino acid between tested compound compared to amoxicillin as the control marked with underline (Table 6). The best interacting compound for *S. aureus* TyRS is myricetin and for the C30 is epicatechin with the binding affinity -9,7 kcal/mol and -7,9 kcal/mol respectively. The two compounds with the highest binding affinity for C30 (Luteonin-7-O-rutinoside and Hesperidin) did not pass the drug-likeness prediction, so epicatechin with the third highest binding affinity was the best compound for C30 inhibitor. Both myricetin and amoxicillin interact with ASP40 and ASP80 amino acid, while in epicatechin the same interacting compound compared to control were TYR 129 and GLN 165 (Figure 3). For the *E. coli,* the target protein is GyrB and DDl and the best compound is nepetin and hispidulin with binding affinity -8.4 Kcal/mol and -7,0 Kcal/mol respectively, the interaction detail shown in Table 6. Compared to amoxicillin, nepetin also interact with GLY

77, ILE 78, PRO 79 amino acid. While hispidulin interacts with same ALA 14, MET 154, TYR 212 amino acid to amoxicillin (Figure 3).

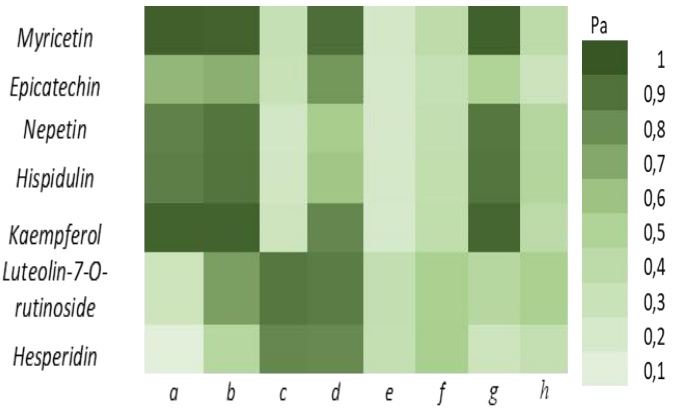

Figure 2: Probable biological activity of several extracted compounds. a. Peroxidase inhibitor; b. Kinase inhibitor; c. Alpha glucosidase inhibitor; d. Antioxidant; e. Antibiotic; f. Antibacterial; g. Antimutagenic; h. Antimycobacterial

Tyrosyl-tRNA synthetase (TyrRS) and C30 carotenoid dehydrosqualene synthase (C30) was chosen as a target for anti-*S. aureus* strain model as for the *E. coli* the selected target was GyraseB and D-alanyl-D-alanine ligase. Tyrosyl-tRNA synthetase (TyrRS) is a type of aminoacyl tRNA synthetase (AaRS) that is currently seen as anti-gram-positive bacteria through protein synthesis blocking, directly affecting bacterial growth and later promoting cell death.[35] While the rationale behind the use of C30 as a target protein was because *S. aureus* produced C30 carotenoid pigment including staphyloxanthin (SPX) which functions as an antioxidant and protects them from oxidative stress.[33] While the *E. coli* strain target GyrB is an important type II topoisomerase that couples the free energy of ATP hydrolysis by introducing negative supercoils into relaxed plasmid DNA.[36] While DDl is an ATP-grasp enzyme that played an important role to facilitate bacterial cell wall synthesis by catalyzing ATP-dependent formation of the d-alanyl–d-alanine dipeptide.[37] Inhibiting GyrB and DDl activity consequently impairs many important physiological processes. Expected inhibiting pathway for both *E. coli* and *S. aureus* illustrated in Figure 4.

Table 4: Interpretation LC MS/MS Spectra Pine Flower Extract

No.	Retention Time (Minutes)	Molecule Name	Chemical Formula	Molecular Structures
1	6.835	(-) Epicatechin (2R,3R)-2-(3,4-dihydroxyphenyl)-3,4-dihydro-2H-chromene-3,5,7-triol	$C_{15}H_{14}O_6$	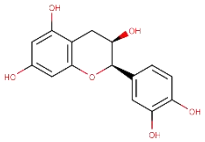
2	8.593	Nepetin 2-(3,4-dihydroxyphenyl)-5,7-dihydroxy-6-methoxychromen-4-one	$C_{16}H_{12}O_7$	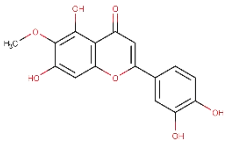
3	10.308	Myricetin 3,5,7-trihydroxy-2-(3,4,5-trihydroxyphenyl)chromen-4-one	$C_{15}H_{10}O_8$	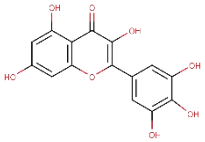
4	11.300	Hispidulin 5,7-dihydroxy-2-(4-hydroxyphenyl)-6-methoxychromen-4-one	$C_{16}H_{12}O_6$	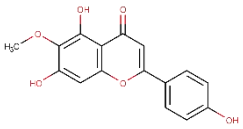
5	12.045	Kaempferol 3,5,7-trihydroxy-2-(4-hydroxyphenyl)chromen-4-one	$C_{15}H_{10}O_6$	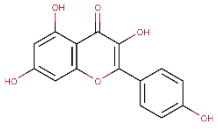
6	16.791	Luteolin-7-O-rutinoside 2-(3,4-dihydroxyphenyl)-5-hydroxy-7-[(3R,4S,5S,6R)-3,4,5-trihydroxy-6-[[(2S,3S,5S,6S)-3,4,5-trihydroxy-6-(hydroxymethyl)oxan-2-yl]oxymethyl]oxan-2-yl]oxychromen-4-	$C_{27}H_{30}O_{16}$	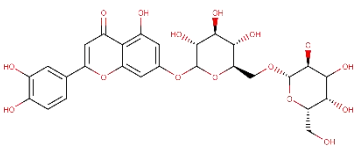

		one		
7	18.063	Hesperidin (2S)-5-hydroxy-2-(3-hydroxy-4-methoxyphenyl)-7-[(2S,3R,4S,5S,6R)-3,4,5-trihydroxy-6-[[(2R,3R,4R,5R,6S)-3,4,5-trihydroxy-6-methyloxan-2-yl]oxymethyl]oxan-2-yl]oxy-2,3-dihydrochromen-4-one	$C_{28}H_{34}O_{15}$	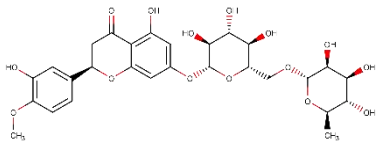

Table 5: Drug-Likeness Prediction of Several Compounds Extracted from *P. Merkusii*

No	Compound (s)	PubChem Id	Formula	Lipinski Parameters				Violation	Bioavailability
				MW (g/mol)	mLogP	nON	nOHNH		
1	Myricetin	5281672	$C_{15}H_{10}O_8$	318.24	-1.08	8	6	1	0.55
2	Epicatechin	72276	$C_{15}H_{14}O_6$	290.27	0.24	6	5	0	0.55
3	Nepetin	5317284	$C_{16}H_{12}O_7$	316.26	-0.31	7	4	0	0.55
4	Hispidulin	5281628	$C_{16}H_{12}O_6$	300.26	0.22	6	3	0	0.55
5	Kaempferol	5280863	$C_{15}H_{10}O_6$	286.24	-0.03	6	4	0	0.55
6	Luteolin-7-O-rutinoside	14032966	$C_{27}H_{30}O_{16}$	610.52	-4.16	15	10	3	0.17
7	Hesperidin	10621	$C_{28}H_{34}O_{15}$	610.56	-3.04	15	8	3	0.17

Table 6: In-Depth Molecular Docking Analysis

No.	Protein Target	Compound Name	Binding Affinity (kcal/mol)	Amino Acid
1	*S. aureus*, TyRS	Amoxicilin (control)	-8,5	Aspartic acid 40; Histidine 47; Glycine 49; Histidine 50; Proline 53; Aspartic acid 80; Tyrosine 170; Glutamine 174.
		Myricetin	-9,7	Aspartic acid 40; Histidine 50; Leucine 70; Aspartic acid 80; Lysine 84; Aspartic acid 177.
		Nepetin	-9,6	Leucine 70; Aspartic acid 80; Lysine 84; Aspartic acid 177.
		Luteonin-7-O-rutinoside	-9,5	Tyrosine 36; Glycine 49; Leucine 70; Aspartic acid 80; Lysine 84; Asparagine 124; Glycine 193; Aspartic acid 195; Glutamine 196.
2	*S. aureus*, C 30	Amoxicilin (control)	-7,1	Arginine 45; Tyrosine129; Glutamine 165.
		Luteonin-7-O-rutinoside	-9,1	Histidine 18; Aspartic acid 52; Aspartic acid 114; Tyrosine 129; Glutamine 165; Asparagine 168; Arginine 171; Aspartic acid 176; Asparagine 179; Tyrosine 183.
		Hesperidin	-8,9	Arginine 45; Valine 111; Aspartic acid 114; Tyrosine 129; Valine 133; Glutamine 165; Aspartic acid 176; Asparagine 179;

ISSN 2616-0684 (Print)
ISSN 2616-0692 (Electronic)

				Aminoethylglycine 181.
		Epicatechin	-7,9	Valine 111; Aspartic acid 114; Tyrosine 129; Glutamine 165; Asparagine 168; Aspartic acid 176.
3	*E. coli*, gyrase B	Amoxicilin (control)	-7,3	Asparagine 46; Aspartic acid 73; Glycine 77; Isoleucine 78; Proline 79; Isoleucine 94; Valine 97.
		Nepetin	-8,4	Valine 43; Glutamic acid 50; Arginine 76; Glycine 77; Isoleucine 78; Proline 79; Valine 120.
		Myricetin	-8,3	Alanine 43; Glutamic acid 50; Aspartic acid 73; Arginine 76; Glycine 77; Isoleucine 78; Proline 79; Threonine 165.
		Luteonin-7-O-rutinoside	-8,3	Asparagine 46; Alanine 47; Glutamic acid 50; Glycine 77; Isoleucine 78; Proline 79.
4	*E. coli*, DDl	Amoxicilin (control)	-6,4	Alanine 14; Methionine 154; Tyrosine 212; Glutamic acid 213.
		Hispidulin	-7	Alanine 14; Methionine 154, Phenylalanine 209; Tyrosine 212.
		Nepetin	-6,8	Valine 152; Glycine 153, Methionine 154; Tyrosine 212; Aspartic acid 211.
		Myricetin	-6,2	Alanine 14; Glycine 15; Methionine 154; Tyrosine 212.

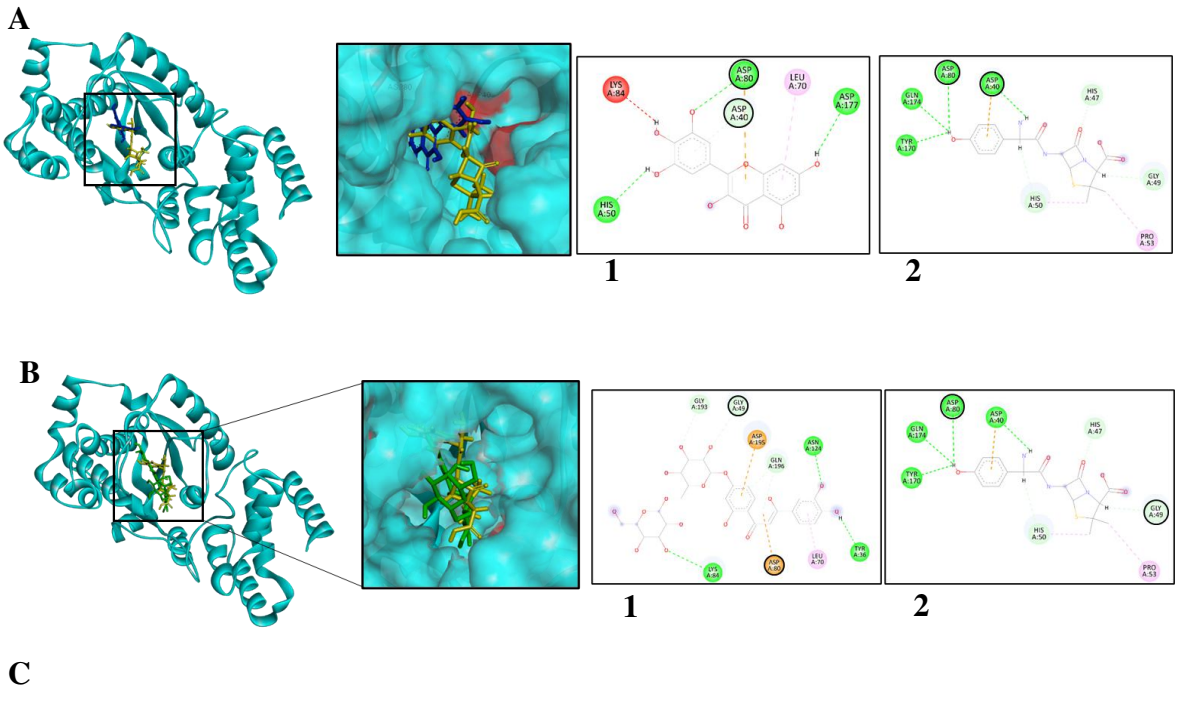

ISSN 2616-0684 (Print)
ISSN 2616-0692 (Electronic)

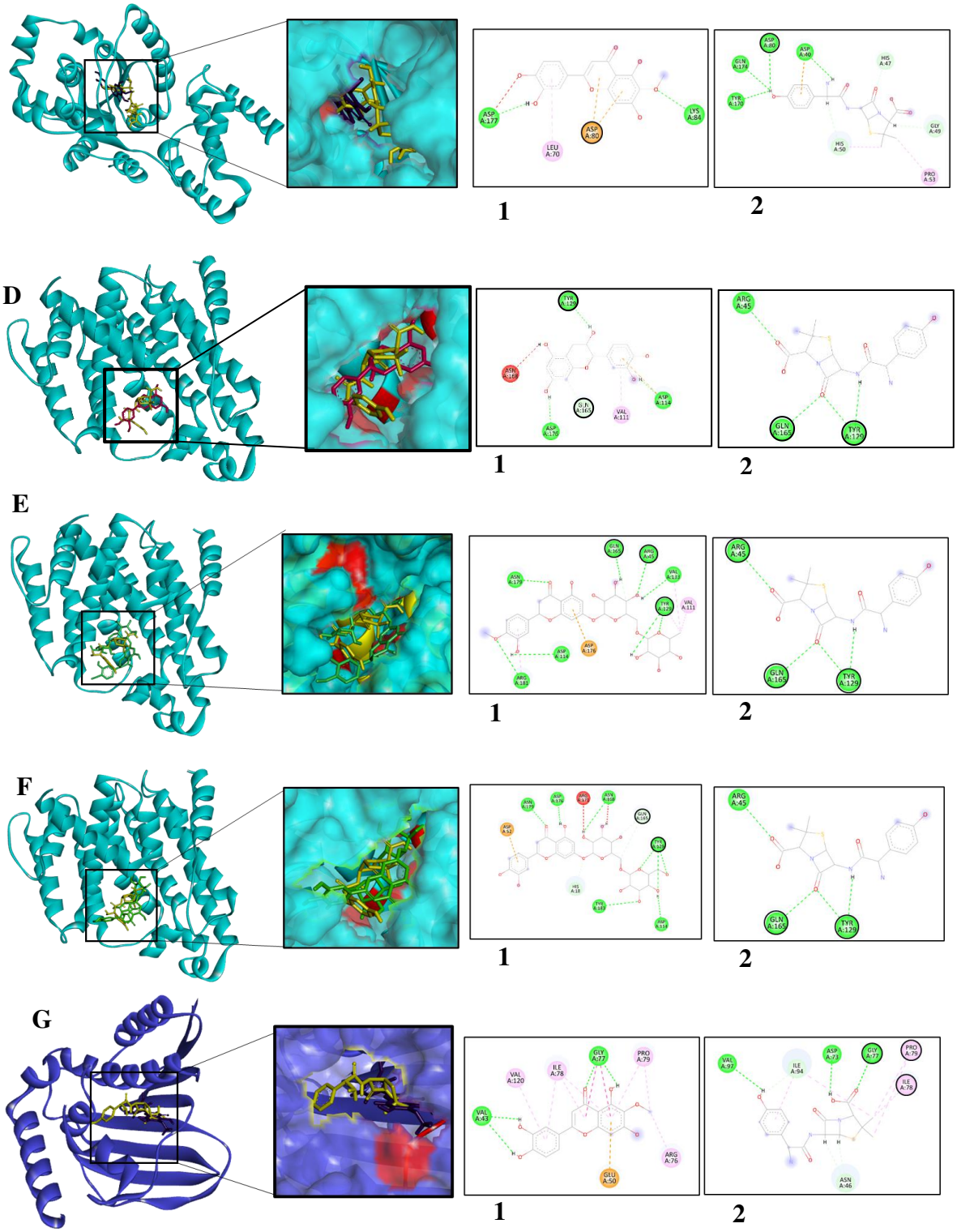

ISSN 2616-0684 (Print)
ISSN 2616-0692 (Electronic)

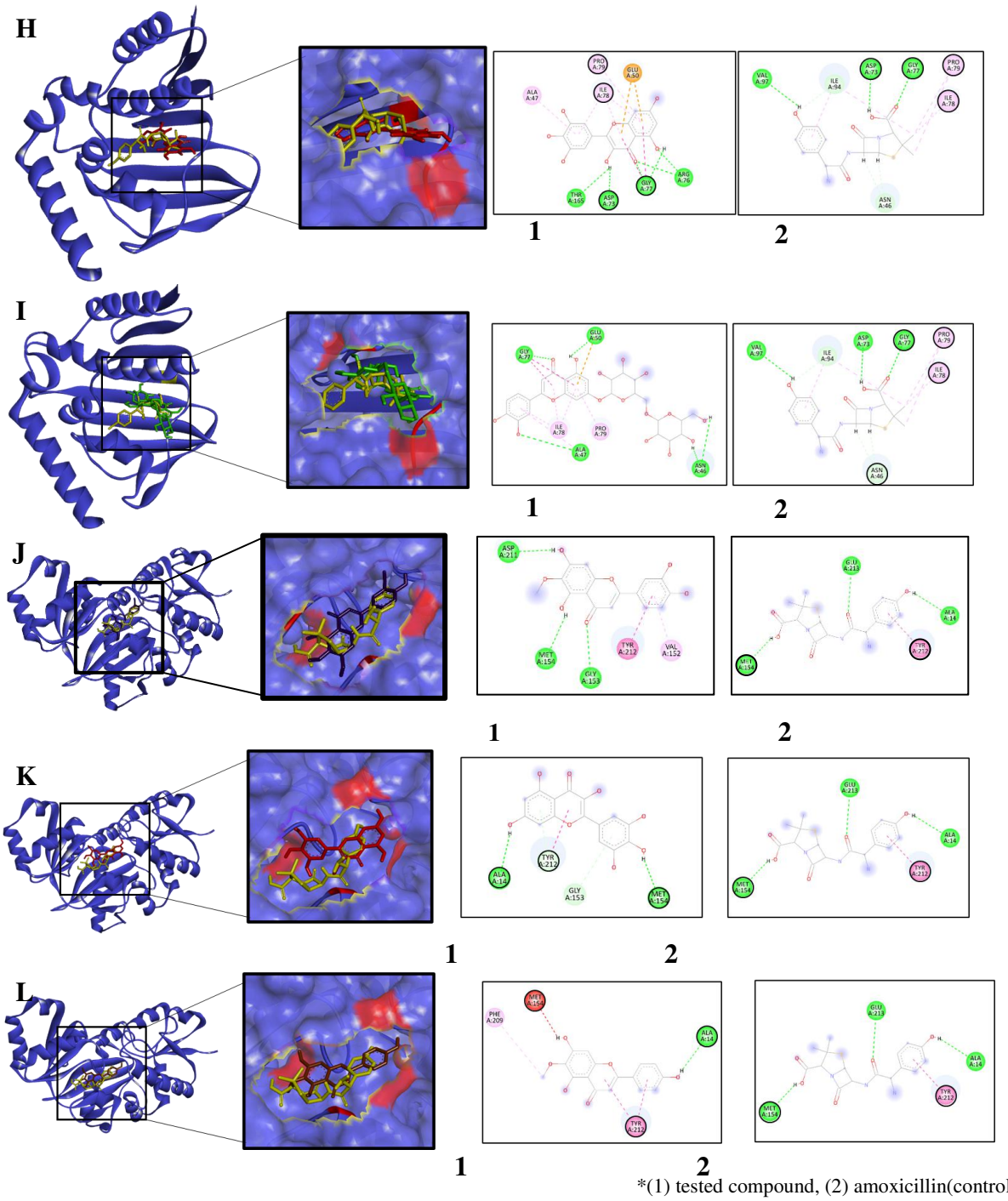

Figure 3: Molecular docking visualization comparing tested compounds with amoxicillin as control. A. Myricetin & TyRS; B. Luteonin-7-O-rutinoside & TyRS; C. Nepetin & TyRS; D. Epicatechin & C30; E. Hesperidin & C30; F. Luteonin-7-O-rutinoside & C30; G. Nepetin & GyraseB; H. Myricetin & GyraseB; I. Luteonin-7-O-rutinoside & GyraseB; J. Nepetin & DDl; K. Myricetin & DDl; L. Hispidulin & DDl.

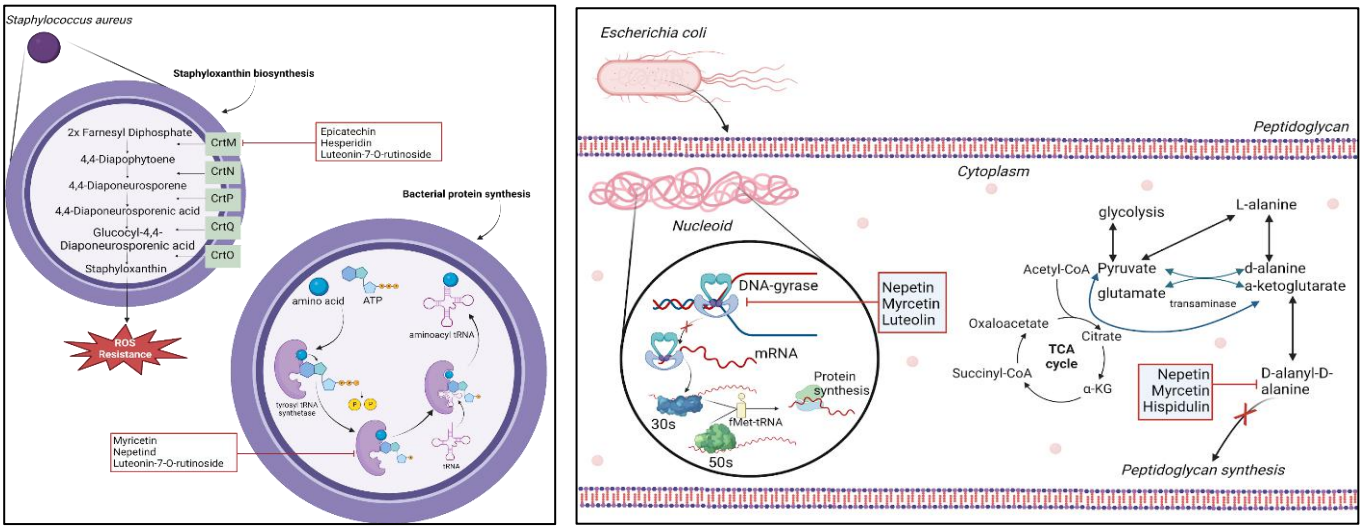

Figure 4: Conceptual representation of the interaction pathway between the inhibiting compound with highest binding affinity and the key protein target. b. *Staphylococcus aureus*; b. *Escherichia coli*

Molecular dynamic simulation

Molecular dynamic (MD) simulation offers new insight into protein motion since molecular recognition and compound binding are very dynamic processes resolving molecular docking limitations that only allow direct visualization.[38] MD simulation trajectory calculated several geometric quantities that can be further elaborated on the underlying mechanism of the observed interactions including root mean square difference (RMSD) and RMS fluctuations (RMSF). RMSD illustrates the difference between the sampled structure to their reference structure during the simulation period. The RMSD value is presented in Angstrom (Å) unit with a value under 2Å considered relevant and accurate.[39,40] MD result for the compounds with the highest binding affinity for *S. aureus* TyRs indicating good molecular stability, especially for Myricetin with a rather stable fluctuation right under the dashed line as the threshold. For the C30 as a target, all compounds indicate relevant and accurate RMSD results as all graph average values at 1.25Å during the simulation period. The RMSD value for *E. coli* GyrB fluctuated during the simulation period, but the graph for all compounds remained under the threshold and stabilized over time. MD result for the compound with the highest binding affinity against DDl displays extreme ups and downs, though, Myricetin remains stable during the simulation period (Figure 5).

Conclusion

According to the antibacterial disk diffusion assay, pine flower extract exhibited the largest inhibition zone on average (for both *S. aureus* and *E. coli*). Further analysis using LC MS/MS for the pine tree parts extract identified several compounds as myricetin, epicatechin, nepetin, hispidulin, kaempferol, luteolin-7-O-rutinoside, and hesperidin. The underlying mechanism of pine tree antibacterial activity was then predicted using a molecular docking analysis. The result indicates that *S. aureus* TyRS best inhibiting compound is myricetin, while the C30 is epicatechin. For the *E. coli* Gyrase B, the best compound was nepetin, as for the DDl, hispidulin was the best inhibiting compound

Conflict of Interest

The authors declare no conflict of interest.

Authors' Declaration

The authors hereby declare that the work presented in this article is original and that any liability for claims relating to the content of this article will be borne by them.

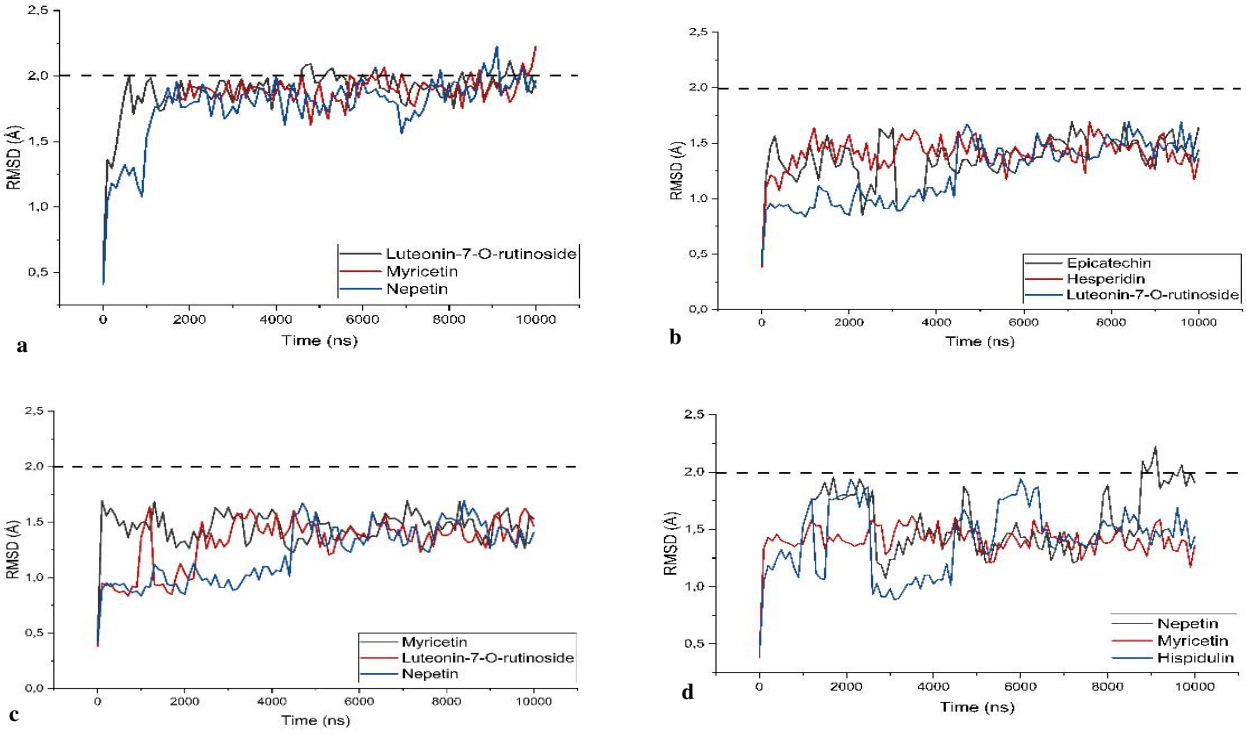

Figure 5: MD Results Indicating the Dynamics of the Structure. a. *S. aureus* TyRS, b. *S. aureus* C30, c. *E. coli* gyrase B, d. *E. coli* D-Alanin Ligase

Acknowledgments

The authors would like to thank the The Ministry of Education, Culture, Research, and Technology of the Republic of Indonesia for support through "Penelitian Dasar Unggulan Perguruan Tinggi 2022".

References

1. Fair RJ, Tor Y. Antibiotics and Bacterial Resistance in The 21st Century. Perspect Med Chem. 2014;1(6):25–64.
2. Chandra H, Bishnoi P, Yadav A, Patni B, Mishra AP, Nautiyal AR. Antimicrobial Resistance and the Alternative Resources with Special Emphasis on Plant-Based Antimicrobials-A Review. Plants. 2017;6(2):16-21.
3. Chitra Jain; Shivani Khatana; Rekha Vijayvergia. Bioactivity of Secondary Metabolites of Various Plants: a Review. Int J Pharm Sci Res. 2019;10(2):494–504.
4. Inayah N, Masruri M. Free-Radical Scavenging Activity (FRSA) of Secondary Metabolite Extracted from Indonesian Eucheuma spinosum. Alchemy J Chem. 2021;9(1):1–6.
5. Azizah FR, Ikhtiarini N, Masruri M, Srihardyastutie A, Rahman MF. Characterization of Cellulose Isolated from Pinewood Waste (*Pinus merkusii*). AIP Conf Proc. 2022;2513(1):030002.
6. Permatasari ND, Witoyo JE, Masruri, Yuwono SS, Widjanarko SB. In Silico Screening of *Syzygium myrtifolium* Flavonoid Compounds as Anti-Bacterial Activity: In Silico Screening of *Syzygium myrtifolium* Flavonoid Compounds. J Trop Life Sci. 2022;12(3):299–306.
7. Dash S, Behera PM, Mandal U, Nayak R, Parida S, Mahalik G, et al. Potential Medicinal Plants of Centurion University of Technology and Management, Bhubaneswar and Their Medicinal Uses. J Med Plants Stud. 2021;9(3):251–8.
8. Amaliyah S, Sabarudin A, Masruri M, Sumitro SB. Characterization and Antibacterial Application of Biosynthesized Silver Nanoparticles Using *Piper Retrofractum* Vahl Fruit Extract as Bioreductor. J Appl Pharm Sci. 2022;12(3):103–14.
9. Dehghan EMJ, Bozorgmehr A, Hajjari SN, Sadat Sombolestani A, Sadeghizadeh M. Review of New Insights Into Antimicrobial Agents. Cell Mol Biol. 2017;1(12):102-108.
10. Indriatie R, Mudaliana S, Hapsari FR, Masruri M. Phytochemistry and Antibacterial Activity Evaluation of Genitri (*Elaeocarpus ganitrus*). IOP Conf Ser Mater Sci Eng. 2020;833(1):012016.
11. Gruszczyk J, Olivares-Illana V, Nourikyan J, Fleurie A, Béchet E, Gueguen-Chaignon V, et al. Comparative Analysis of the Tyr-Kinases CapB1 and CapB2 Fused to Their Cognate Modulators CapA1 and CapA2 from *Staphylococcus aureus*. PLoS ONE. 2013;8(10).
12. Furubayashi M, Saito K, Umeno D. Evolutionary Analysis of The Functional Plasticity of *Staphylococcus aureus* C30 Carotenoid Synthase. J Biosci Bioeng. 2014;117(4):431–6.
13. Saíz-Urra L, Cabrera MA, Froeyen M. Exploring the Conformational Changes of the ATP Binding Site of gyrase B from *Escherichia coli* Complexed with Different Established Inhibitors by Using Molecular Dynamics Simulation: Protein–ligand Interactions in the Light of The Alanine Scanning and Fre. J Mol Graph Model. 2011;29(5):726–39.
14. Júnior JRP, Caruso ÍP, de Sá JM, Mezalira TS, de Souza Lima D, Pilau EJ, et al. Characterization of Secondary Structure and Thermal Stability by Biophysical Methods of the D-alanyl,D-alanine Ligase B Protein from *Escherichia coli*. Protein Pept Lett. 2022;29(5):448–59.

15. Bai H, Xue X, Hou Z, Zhou Y, Meng J, Luo X. Antisense Antibiotics: A Brief Review of Novel Target Discovery and Delivery. Curr Drug Discov Technol. 2014;7(2):76–85.
16. Nurdin KE, Ratna L, Olla Y, Feoh SF, Dwi A, Galla P, Jonison EFF, Kambuno NT. Effectivity Test of 96% from Soe (*Citrus sinensis* L.) Sweet Orange Rind Ethanol Extract as Biolarvaside. J INFO Kesehat. 2019;17(2):176–83.
17. Astuti P, Rollando R, Wahyuono S, Nurrochmad A. Antimicrobial activities of isoprene compounds produced by an endophytic fungus isolated from the leaves of *Coleus amboinicus* Lour. J Pharm Pharmacogn Res. 2020;8(4):280–9.
18. Hariono M, Nuwarda RF, Yusuf M, Rollando R, Jenie RI, Al-Najjar B, Julianus J, Putra KC, Nugroho ES, Wisnumurti YK, Dewa SP, Jati BW, Tiara R, Ramadani RD, Qodria L, Wahab HA. Arylamide as Potential Selective Inhibitor for Matrix Metalloproteinase 9 (MMP9): Design, Synthesis, Biological Evaluation, and Molecular Modeling. J Chem Inf Model. 2020;60(1):349–59.
19. Iskandar D, Widodo N, Warsito W, Masruri M, Rollando R, Warsidah W, Antang, YPP. Proposed Functional Activity of Bioactive Compounds from *Spatholobus littoralis* Hassk in LC-MS-MS and Silico Studies. Mater Sci Forum. 2022;1061:181–6.
20. Yuniati Y, Yuliati L, Monica E, Rollando R. Discovering anticancer compound of ethyl acetate extract from RL1 code endophytic fungi culture derived by *Phyllanthus niruri* Linn leaves through cell cycle modulation in T47d cells. IOP Conf Ser Mater Sci Eng. 2019;509:012157.
21. Udhwani T, Mukherjee S, Sharma K, Sweta J, Khandekar N, Nayarisseri A, Singh SK. Design of PD-L1 Inhibitors for Lung Cancer. Bioinformation. 2019;15(2):139–50.
22. Hariono M, Rollando R, Karamoy J, Hariyono P, Atmono M, Djohan M, Wiwy W, Nuwarda R, Kurniawan C, Salin N, Wahab H. Bioguided Fractionation of Local Plants against Matrix Metalloproteinase9 and Its Cytotoxicity against Breast Cancer Cell Models: In Silico and In Vitro Study. Mol Basel Switz. 2020;25(20).
23. Hariono M, Rollando R, Yoga I, Harjono A, Suryodanindro A, Yanuar M, Gonzaga T, Parabang Z, Hariyono P, Febriansah R, Hermawansyah A, Setyani W, Wahab H. Bioguided Fractionation of Local Plants against Matrix Metalloproteinase9 and Its Cytotoxicity against Breast Cancer Cell Models: In Silico and In Vitro Study (Part II). Mol Basel Switz. 2021;26(5):1464.
24. Widyananda MH, Puspitarini S, Rohim A, Khairunnisa FA, Jatmiko YD, Masruri M, Widodo N. Anticancer Potential of Turmeric (*Curcuma longa*) Ethanol Extract and Prediction of its Mechanism Through the AKT1 Pathway. F1000Research 2022 111000. 2022;11:1000.
25. Rollando R, Warsito W, Masruri M, Widodo N. Potential matrix metalloproteinase-9 inhibitor of aurone compound isolated from *Sterculia quadrifida* leaves: *In-vitro* and *in-silico* studies. Res J Pharm Technol. 2022;15(11):5250–4.
26. Rollando R, Warsito W, Masruri M, Widodo W. *Sterculia foetida* Leaf Fraction Against Matrix Metalloproteinase-9 Protein and 4T1 Breast Cancer Cells: In-Vitro and In-Silico Studies. Trop J Nat Prod Res. 2021;5(1):113–21.
27. Rollando R, Warsito W, Masruri M, Widodo W. *Pterygota alata* (Roxb.) R.Br. Bark Fraction Induced Intrinsic Apoptotic Pathway in 4T1 Cells by Decreasing Bcl-2 and Inducing Bax Expression. Pak J Biol Sci PJBS. 2021;24(2):172–81.
28. Rollando R, Warsito W, Masruri M, Nashi W. Antibacterial, Antioxidant, and Cytotoxic Flavonoid Compound from *Sterculia quadrifida* Leaves. Trop J Nat Prod Res. 2021;5(11):1979–85.
29. Hussein RA, El-Anssary AA, Hussein RA, El-Anssary AA. Plants Secondary Metabolites: The Key Drivers of the Pharmacological Actions of Medicinal Plants. Herb Med. 2018;8(11):139-145.
30. Breijyeh Z, Jubeh B, Karaman R. Resistance of Gram-Negative Bacteria to Current Antibacterial Agents and Approaches to Resolve It. Mol. 2020;25(6):1340.
31. Epand RM, Walker C, Epand RF, Magarvey NA. Molecular Mechanisms of Membrane Targeting Antibiotics. Biochim Biophys Acta BBA - Biomembr. 2016;1858(5):980–7.
32. Xie Y, Yang W, Tang F, Chen X, Ren L. Antibacterial Activities of Flavonoids: Structure-Activity Relationship and Mechanism. Curr Med Chem. 2014;22(1):132–49.
33. Hatano T, Kusuda M, Inada K, Ogawa TO, Shiota S, Tsuchiya T, Takasi Y. Effects of Tannins and Related Polyphenols on Methicillin-Resistant *Staphylococcus aureus*. Phytochemistry. 2005;66(17):2047–55.
34. Lipinski CA, Lombardo F, Dominy BW, Feeney PJ. Experimental and Computational Approaches to Estimate Solubility and Permeability in Drug Discovery and Development Settings. Adv Drug Deliv Rev. 2001;46(3):3–26.
35. Delarue M. Aminoacyl-tRNA Synthetases. Curr Opin Struct Biol. 1995;5(1):48–55.
36. Gross CH, Parsons JD, Grossman TH, Charifson PS, Bellon S, Jernee J, Dwyer M, Chambers SP, Markland W, Botfield M, Raybuck SA. Active-Site Residues of *Escherichia coli* DNA Gyrase Required in Coupling ATP Hydrolysis to DNA Supercoiling and Amino Acid Substitutions Leading to Novobiocin Resistance. Antimicrob Agents Chemother. 2003;47(3):1037–46.
37. Pederick JL, Thompson AP, Bell SG, Bruning JB. D-alanine–D-alanine Ligase as a Model for the Activation of ATP-Grasp Enzymes by Monovalent Cations. J Biol Chem. 2020;295(23):7894–904.
38. Cheng X, Ivanov I. Molecular Dynamics. 2012;243–85.
39. Hevener KE, Zhao W, Ball DM, Babaoglu K, Qi J, White SW, Lee RE. Validation of Molecular Docking Programs for Virtual Screening Against Dihydropteroate Synthase. J Chem Inf Model. 2009;49(2):444–60.
40. Castro-Alvarez A, Costa AM, Vilarrasa J. The Performance of Several Docking Programs at Reproducing Protein–Macrolide-Like Crystal Structures. Mol. 2017;22(1):136.